J. Coat. Technol. Res., **19** (5) 1345–1355, 2022
https://doi.org/10.1007/s11998-022-00626-w

Polymeric aziridines as benign crosslinkers for water-based coating applications

A. J. P. Bückmann, Q. Chen, G. C. Overbeek, P. J. M. Stals, D. van der Zwaag

Received: 1 November 2021 / Revised: 11 February 2022 / Accepted: 19 February 2022

Abstract Polymeric aziridines are introduced as a new class of low toxicity two-component crosslinkers for carboxylic resins. Using a combination of industry-standard tests and modern biotechnological approaches, the non-genotoxic nature of these compounds was demonstrated. Mechanical analysis of acrylic films formulated with these polymeric aziridines demonstrated that the high crosslink densities typical for classical aziridine chemistry could be attained. Furthermore, distribution of crosslinker molecules in both wet formulation and dried coating could be controlled by adjusting the stabilizing group of the polymeric aziridine. By tuning this stabilization mechanism, we demonstrated customized functional performance for different coating applications.

Keywords Aziridines, Crosslinking, Waterborne coatings, Morphology, Additives

Introduction

Crosslinkers represent one of the most important classes of additives in the coating industry, used widely to improve the chemical and mechanical resistances of coating systems as well as to improve adhesion.

Crosslinkers are typically divided into two categories: one-component (1K) crosslinkers and two-component (2K) crosslinkers. The first category represents crosslinkers already present in the formulation during storage, usually in a dormant state in which they do not react with other components, until triggered by for instance a change in pH, temperature or UV-irradiation. It then crosslinks another component of the formulation, usually the resin. The latter category represents crosslinkers which are added to a formulation a limited time before applying it to a substrate, and importantly, in which case the total formulation has a limited stability before gelation or loss of performance occurs.

In general, 2K crosslinking improves coating systems to a larger extent than 1K approaches. Such improvement is particularly relevant for waterborne coating systems,[1] in which the performance of the coating binder is often perceived as inferior to that of their more traditional solventborne counterparts.[2] This is typically attributed to the presence of water-sensitive parts in the composition, such as surfactants and incorporated ionic (stabilizing) groups (Fig. 1). Removing those groups by crosslinking during and after the drying and coalescence process will significantly improve properties.

In chemical terms, the most relevant 2K crosslinkers for waterborne systems fall into one of three categories: isocyanates, carbodiimides and aziridines. Isocyanates are known to be very efficient crosslinkers and react with custom-designed binders with a high hydroxyl content to offer an optimal performance. Polycarbodiimides[3,4] and polyaziridines react with the carboxylic acids inherently present in the vast majority of waterborne resins as dispersing and stabilizing moieties (Fig. 1). A second favorable property of polycarbodiimides and polyaziridines is their long pot-life, which significantly improves the ease of handling for the user.

Aziridine crosslinkers represent a good balance between reliability, versatility and reactivity that one might look for in a crosslinker for waterborne systems.[4,5] The reaction mechanism of aziridines with carboxylic acids is displayed in Scheme 1. In this two-step process the basic aziridine is in first instance protonated, after which in the second step the depro-

A. J. P. Bückmann, Q. Chen, G. C. Overbeek (✉),
P. J. M. Stals, D. van der Zwaag
Covestro Coating Resins BV, Sluisweg 12, 5145PE
Waalwijk, The Netherlands
e-mail: ad.overbeek@covestro.com

tonated carboxylic acid preferably attacks the least-substituted carbon atom of the aziridine ring, yielding a secondary amine which is known in some instances to tautomerize to a β-hydroxy amide.

Mutagenicity is an unfavorable aspect of the toxicity of classical aziridines[6] (Fig. 2). Therefore, we set out to design a new polyaziridine crosslinker which was no longer mutagenic. Our final design differed from the classical aziridines in several aspects; first of all a polymeric backbone was introduced, yielding a significantly higher molecular weight than the classical aziridines, and second we utilized urethane bonds to connect the aziridine groups to this backbone.

Synthesis of this new category of crosslinkers proceeded in a two-step approach;[7] in the first step we reacted propylene imine with an epoxide functional compound, resulting in a β-hydroxyalkyleneaziridine intermediate. This intermediate was subsequently reacted, together with a stabilizing moiety, to a polyfunctional isocyanate to obtain the polymeric aziridine crosslinker **A-3** (Fig. 3), commercially available as Neoadd^{TM} PAX-521 and Neoadd^{TM} PAX-523, and slightly more hydrophilic **A-4**, commercially available as Neoadd^{TM} PAX-524. By omitting the stabilizing moiety entirely, reference compound **A-5** was synthesized.

Experimental

Materials

Crosslinker **A-1** and laboratory chemicals for synthesis, formulation and analysis were obtained from common laboratory suppliers. Crosslinkers **A-2**, **A-3**, **A-4** and **A-5** were obtained from Covestro AG (previously DSM Coating Resins).

Synthesis

A model acrylic binder with a theoretical T_g of −14°C (according to Flory-Fox equation) was synthesized as follows. A 2-L four-necked flask equipped with a

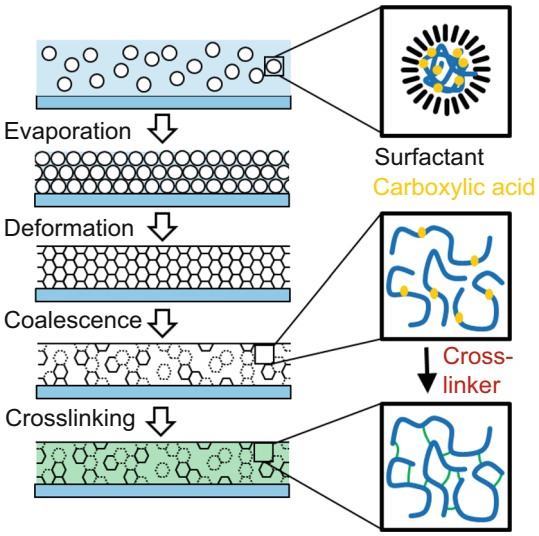

Fig. 1: Film formation process of waterborne systems

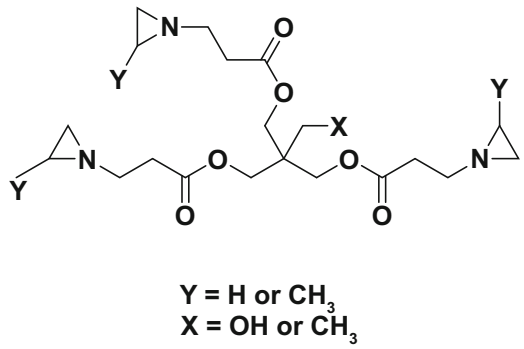

Fig. 2: Schematic depiction of classical aziridine crosslinkers; most common aziridine crosslinkers are pentaerythritol tris[3-(1-aziridinyl)propionate] (Y=H, X=OH; A-1) and trimethylolpropane tris[3-(1-(2-methyl)aziridinyl)propionate] (Y=CH$_3$, X=CH$_3$; A-2)

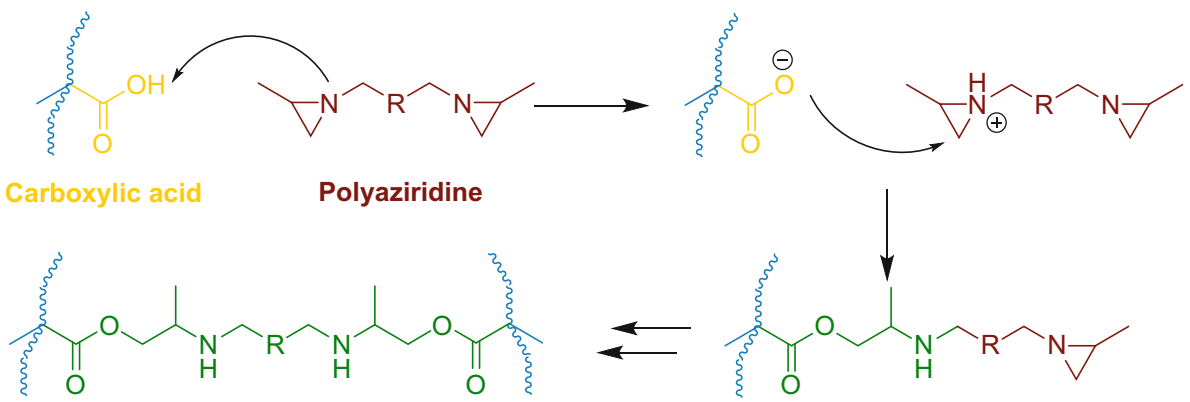

Scheme 1: Generalized mechanism for aziridine crosslinking

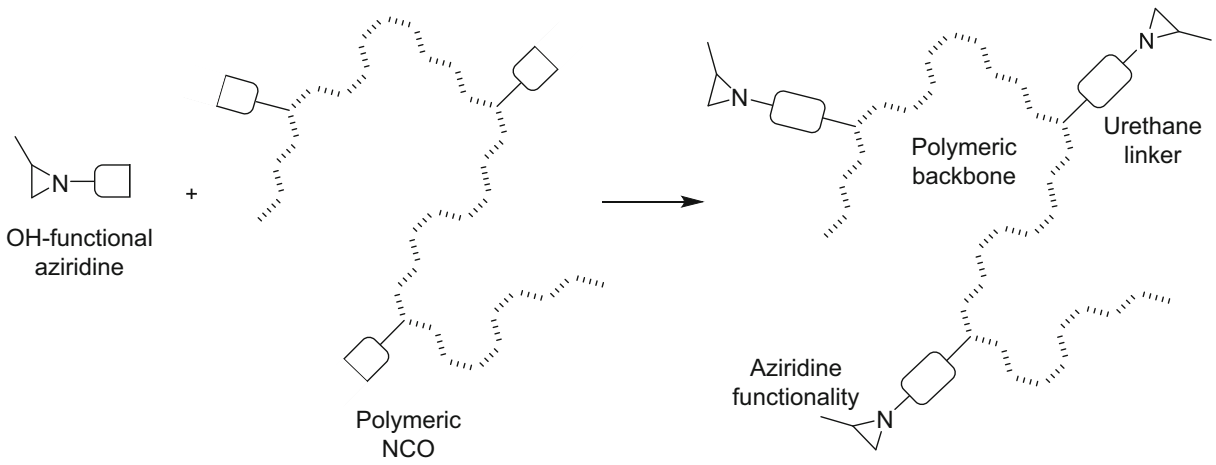

Fig. 3: Synthetic approach for A-3, A-4 and A-5

thermometer and overhead stirrer was charged with sodium lauryl sulphate (30% solids in water, 18.6 grams of solution) and demineralized water (711 grams). The reactor phase was placed under N_2 atmosphere and heated to 82°C. A mixture of demineralized water (112 grams), sodium lauryl sulphate (30% solids in water, 37.2 grams of solution), methyl methacrylate (209.3 grams), n-butyl acrylate (453.56 grams) and methacrylic acid (34.88 grams) was placed in a large feeding funnel and emulsified with an overhead stirrer (monomer feed). Ammonium persulphate (1.75 grams) was dissolved in demineralized water (89.61 grams) and placed in a small feeding funnel (initiator feed). Ammonium persulphate (1.75 grams) was dissolved in demineralized water (10.5 grams), and this solution was added to the reactor phase. Immediately afterwards, 5% by volume of the monomer feed was added to the reactor phase. The reaction mixture then exothermed to 85°C and was kept at 85°C for 5 minutes. Then, the residual monomer feed and the initiator feed were fed to the reaction mixture over 90 minutes, maintaining a temperature of 85°C. After completion of the feeds, the monomer feed funnel was rinsed with demineralized water (18.9 grams) and reaction temperature maintained at 85°C for 45 minutes. Subsequently, the mixture was cooled to room temperature and brought to pH = 7.2 with ammonia solution (6.25 wt.% in demineralized water), and brought to 40% solids with further demineralized water. The particle size (diameter, as determined by DLS) was 55 nm.

Formulation

Coating formulations of crosslinkers **A-2** and **A-3** with the model acrylic binder, as well as a reference non-crosslinked sample, for dynamic mechanical thermal analysis (DMTA) experiments were prepared as follows. Into a 100-mL flask with overhead stirrer, 40 grams of acrylic binder was weighed. Then, 0.02 grams of BYK-346 and 0.2 grams of a 5:1 mixture of demineralized water:Borchigel L75N were added to each formulation. After stirring for 15 minutes, formulations were rested overnight. Subsequently, crosslinkers **A-2** and **A-3** were added to a carboxylate:aziridine stoichiometric amount of 1 : 0.93. Reference sample and sample **A-2** were corrected with the amount of methoxypropyl acetate present in **A-3**. After stirring for 15 minutes and resting for 15 minutes, films of 350 μm wet thickness were cast onto glass coated with release paper using a universal drawbar. Films were cured for 1 hour at room temperature, then for 16 hours at 50°C and taken off the release paper. Prior to the measurements, approximate 12x1 cm strips were cut out of the dry films which were folded 6 to 8 times until a stacked film thickness between 600 and 1000 micron remained. These stacks were placed on the rheometer.

DMTA

The DMTA data of the samples were obtained on a TA Instruments DHR-2 rheometer (TA instruments, New Castle, USA) in oscillation mode, using plate-plate geometry with a plate diameter 8 mm and a frequency of 1 Hz. A temperature range from +180°C to -15°C with a cooling rate of 3° per minute was applied with an initial gap of 500 micrometer. A thermal cover was applied. The stacked free film has been applied on the rheometer at 183°C and pressed together until the required gap of 500 micrometer is obtained, then the measurement is started.

TTS

The time-temperature superposition (TTS) data of the samples have been obtained on a TA Instruments DHR-2 rheometer in oscillation mode, using plate-plate geometry with a plate diameter 8 mm. A

frequency sweep from 5 to 0.1 Hz was applied with five points per decade. Temperature sweep ranged from +100°C to -30°C in steps of 5°, with an initial gap between 600 and 1100 micrometer (depending on film thickness). A constant axial force of 1 N was applied. Initial strain was set to 0.2%, and allowed to vary between 1 and 0.001% during measurement. A dual peltier plate has been used to heat and cool the samples. The TTS Wizard has been used in the generation of the TTS curves. Master curves have been obtained from all measurement data (storage modulus, loss modulus and tan(delta)). Shifts in only X directions have been allowed, and master curves at 25°C have been generated.

Particle size analysis by DLS

Particle size measurements were obtained by Dynamic Light Scattering (DLS) on a Malvern Zetasizer Nano S-90 using disposable cuvettes. Measurements were taken in 90°-mode at 25°C with 2 minute equilibration. The results are the averages of three analyses of 13 individual measurements. The measurement range is approximately 2 nm to 1 μm.

Coating preparation for AFM

For Atomic Force Microscopy (AFM) measurements coating was prepared by drop casting a few mLs of the mixture containing model acrylic resin dispersion and polymeric aziridine crosslinkers (**A-2**, **A-3**, **A-4** or **A-5**) onto Leneta card (Type 2C, Leneta Company, Inc. Mahwah, NJ, USA) and drawing down using a wired rod with a defined thickness of 90 μm. Subsequently the sample was dried overnight in the fume hood at room temperature. Afterwards, the sample was collected and stored in a covered sample box.

AFM measurements

AFM images were obtained under ambient conditions in tapping mode with a Nanoscope V multimode atomic force microscope (Bruker Nano Surfaces, Santa Barbara, CA, USA) using silicon cantilevers with resonance frequencies of 300-400 kHz (model: TESP, Bruker Nano Surfaces).

Formulation for application testing

For application testing with Neorez® R-2005, 6 wt% of a commercial sample of **A-3** (80% solids in methoxy propylacetate) *or* 6 wt% of a commercial sample of **A-4** (50% solids in dipropylene glycol dimethyl ether) was slowly added under vigorous stirring to a mixture of 82 wt% Neorez® R-2005, 17.7 wt% demineralized water and 0.3 wt% ADEKANOL UH-756 (obtained from Adeka Corporation). Samples were applied as a 100 μm wet coating utilizing manual applicators on relevant substrates.

For application testing with Neocryl® XK-117, 2 wt% of a commercial sample of **A-2** *or* 2 wt% of a commercial sample of **A-3** (80% solids in methoxy propylacetate) was slowly added under vigorous stirring to a mixture of 95 wt% Neocryl® XK-117 and 5 wt% of Dowanol^{TM} DPnB (obtained from The Dow Chemical Company). Samples were applied as a 100 μm wet coating utilizing manual applicators on relevant substrates.

Results and discussion

Non-mutagenic aziridines

To establish that polymeric aziridines **A-3**, **A-4** and **A-5** indeed display a more benign toxicity profile than classical aziridines **A-1** and **A-2**, and more specifically that they are indeed non-mutagenic, we analyzed the toxicity of these compounds using three independent tests. First of all, we utilized the ToxTracker® assay from Toxys®. The ToxTracker® assay has been found to perform very well in terms of specificity and sensitivity.[8]

In the ToxTracker® assay the induction levels of biomarkers (Bscl2 and Rtkn) commonly associated with DNA damage and genotoxicity are measured after exposing relevant mammalian reporter cell lines to **A-1** – **A-5**. The assay was performed both in the presence and absence of a S9 rat liver extract, which is commonly applied in *in-vitro* tests as it mimics the hepatic metabolism. Its use is very relevant because some substances are more toxic after metabolic activation, hence this assay measures the possible genotoxic effect of the test compounds as such and also after metabolic activation. Based on the upregulation level of aforementioned biomarkers, compounds are classified as non-genotoxic, mildly genotoxic or genotoxic. As can be seen in Table 1, classical aziridine crosslinkers **A-1** and **A-2** are classified as genotoxic by both biomarkers, in the presence and in the absence of S9 rat liver extract. This is in contrast to novel crosslinkers **A-3, A-4** and **A-5**, which do not display genotoxic response under any condition.

We also performed the industry standard OECD 471 test (bacterial reverse mutation test, commonly known as the AMES test) on compounds **A-2**, **A-3** and **A-4** as well as the independent OECD 487 test (*in-vitro* mammalian cell micronucleus test) on compound **A-3**. As expected, mutagenicity of compound **A-2**, as well as non-genotoxicity and non-mutagenicity of compounds **A-3** and **A-4**, was once again demonstrated by these tests. Therefore, the non-genotoxic and non-mutagenic nature of **A-3** and **A-4** was shown by three independent *in-vitro* tests, investigating different cell-lines of different phylogenetic origin.

Table 1: Induction of biomarkers attributed to DNA damage

Biomarker ->	Without S9 rat liver extract		With S9 rat liver extract	
	Bscl2	Rtkn	Bscl2	Rtkn
A-1				
A-2				
A-3				
A-4				
A-5				

Green color indicates non-genotoxic classification by ToxTracker® assay, orange color indicates a mildly genotoxic classification (not applicable in this table) and red color indicates genotoxic classification.

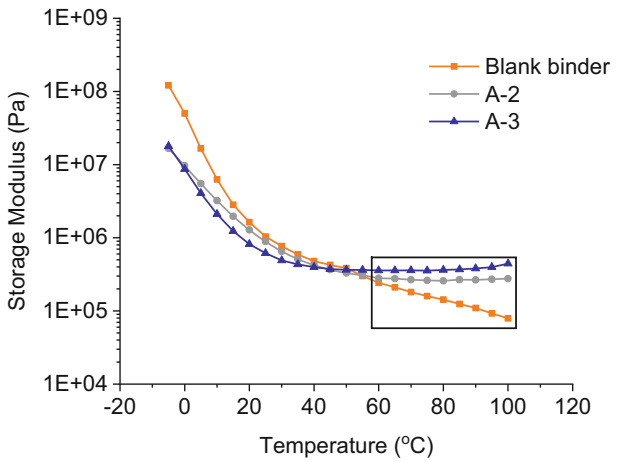

Fig. 4: DMTA analysis of model acrylic binder with $T_{g,theoretical}$ = -14°C, formulated with A-2, A-3 or no crosslinker. Box indicates the high-temperature regime displaying rubbery properties

Analysis of network formation

In addition to its toxicological advantages, retention of typical aziridine crosslinking efficacy is a crucial property of polymeric aziridines. A robust way to demonstrate the formation of a covalently crosslinked network, is the use of Dynamic Mechanical Thermal Analysis (DMTA).[9] In such a measurement, the storage modulus of a non-crosslinked polymer will decrease monotonically at temperatures above its glass transition (T_g). Crosslinked networks on the other hand display a plateau with a modulus slightly increasing with temperature in this regime. Using rubber elasticity theory, the storage modulus value of the plateau can be converted to a crosslink density. Figure 4 shows DMTA measurements of an acrylic model binder formulated with either no crosslinker, with classical aziridine **A-2** or with polymeric aziridine **A-3**. In the high-temperature regime, the expected plateau can be observed for both crosslinked samples. Additionally, crosslink densities for **A-3** are on par with industry standard **A-2**, indicating similar crosslinking efficiencies.

The mechanical response of a polymer network is not universal but rather is rate-dependent, a fact that is important in connecting mechanical behavior to functional properties. Because the type of strain (specifically, its frequency) largely determines its effect on a coating, the rate-dependence of the modulus was investigated. Since it is not practically feasible to measure at extremely low or high shear rates, time-temperature superposition (TTS) was applied to obtain such curves. In a TTS experiment, limited sweeps of the shear rate are performed at different temperatures, followed by computational integration of these sweeps to a single master curve (Fig. 5). TTS mastercurves were acquired for non-crosslinked binder as well as crosslinked films (Fig. 6). In these curves, the high shear rate regime captures both covalent and non-covalent interactions, since the strain has a shorter timescale than the lifetimes of both types of interactions. In the low shear rate regime however, the lifetime of non-covalent interactions is short on the timescale of the strain, resulting in the specific detection of covalent crosslinks. As clearly indicated in the graph, the TTS mastercurves confirm similar crosslinking behavior for classical aziridine crosslinker **A-2** and polymeric aziridine crosslinker **A-3**.

The mechanical analysis outlined here confirms the high reactivity of **A-3**, and proves its ability to form a

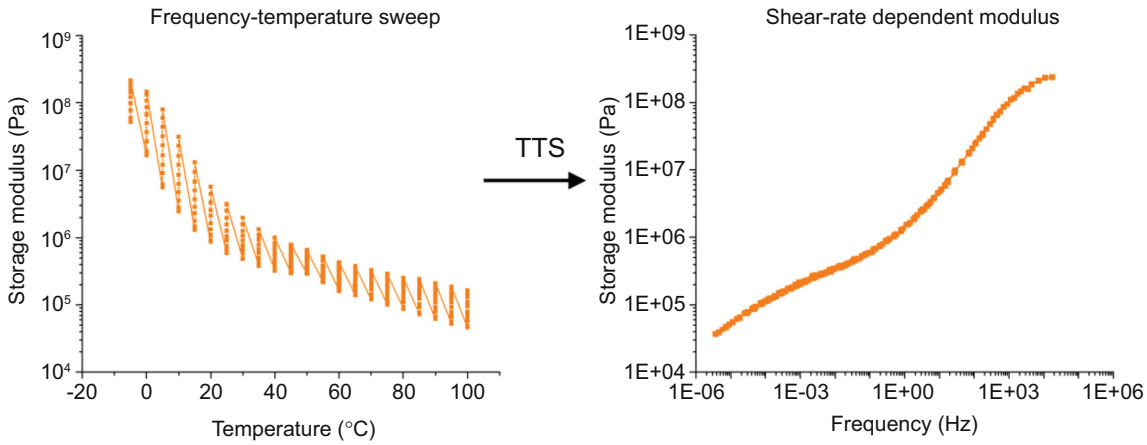

Fig. 5: Acquisition of shear rate sweeps at different temperatures (left panel), and integration of these sweeps through TTS yielding a single master curve (right panel). Curves correspond to model acrylic binder with $T_{g,theoretical}$ = -14°C, without crosslinker

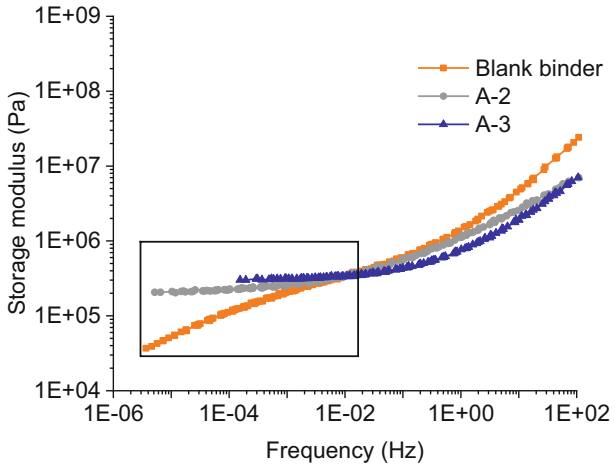

Fig. 6: Shear rate dependent TTS mastercurves. Box indicates low-frequency regime where covalent bonds dominate. Curves correspond to model acrylic binder with $T_{g,theoretical}$ = -14°C, formulated with A-2, A-3 or no crosslinker

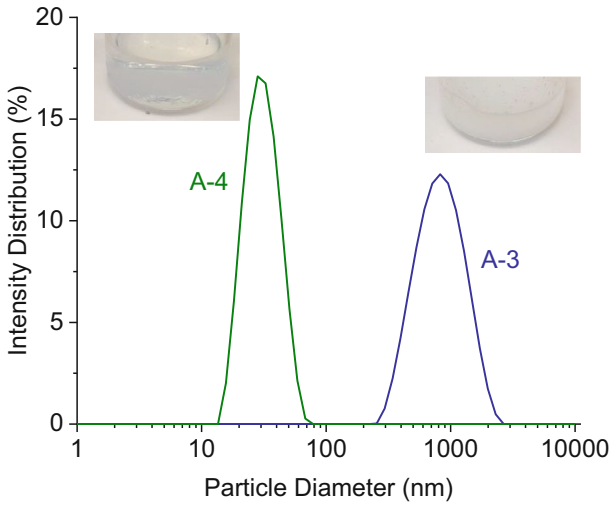

Fig. 7: Intensity distribution vs hydrodynamic diameter for A-3 and A-4, as obtained from DLS measured at a 90° angle. Inset images show the visual difference between aqueous dispersions at higher concentrations of A-3 and A-4

covalent network with carboxylate-functional binders. Such networks typically display improved properties from a durability point of view, including higher elasticity particularly at elevated temperature (evident from its increased storage modulus), reduced creep under load and reduced solubility in a variety of environmental or industrial liquids.

Crosslinker distribution

A key property for crosslinkers used in waterborne systems is their water miscibility and thus compatibility with water-based resins. To test this for **A-3** and **A-4**, we studied the behavior of these two crosslinkers just after dispersion into defined particles in water, using Dynamic Light Scattering (DLS). The measurements in Fig. 7 demonstrate their compatibility with aqueous media. Interesting to note is that the more hydrophilic **A-4** shows significantly smaller particles than **A-3** (~30 nm *vs* ~900 nm), expressing differences in crosslinker distribution that may be exploited to achieve particular properties or performance profiles.

In order to achieve optimal crosslink density and to obtain excellent coating performance, crosslinker molecules should be evenly distributed within the coating to form the crosslinked network. To visualize the distribution of crosslinker molecules after film formation, AFM was used to study surface morphology of coatings prepared using the model acrylic binder formulated with classical low molar mass aziridine **A-2**, stabilized polymeric aziridines **A-3** and **A-4** and non-stabilized polymeric aziridine **A-5**. The obtained AFM

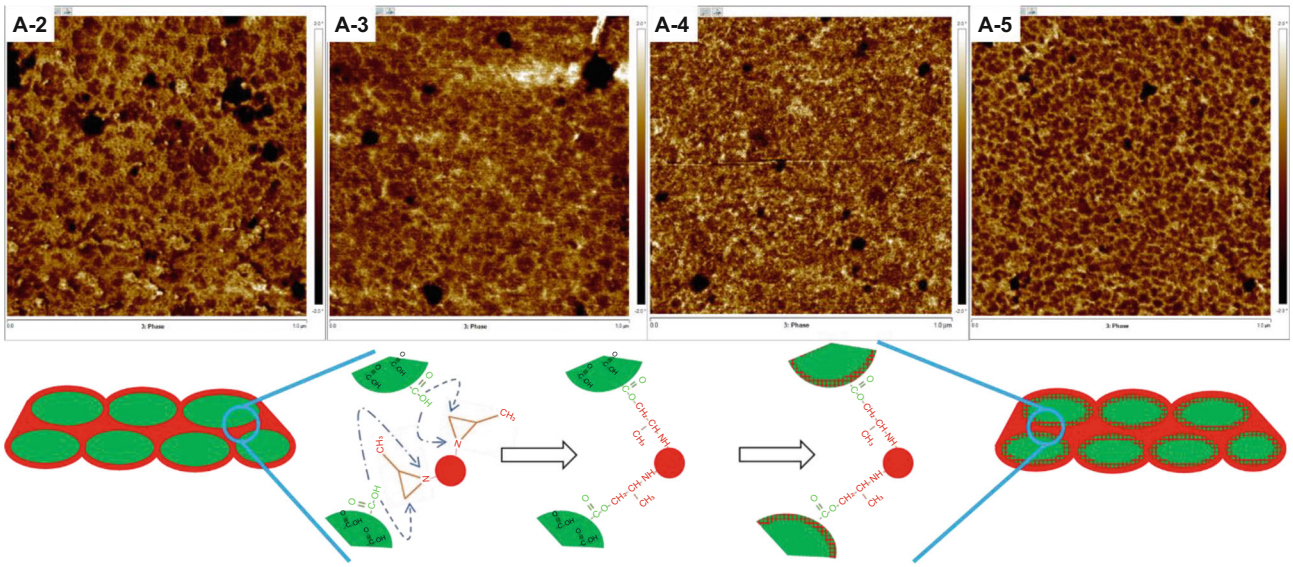

Fig. 8: Tapping mode AFM phase images of coating surfaces prepared from acrylic resin formulated with aziridine crosslinker molecules as indicated in the respective images (upper panels). Image area is 1 × 1 μm^2 for all images. A schematic illustration of crosslinker diffusion in the drying coating, and reaction with carboxyl groups from the acrylic dispersion particles is also shown (lower panel)

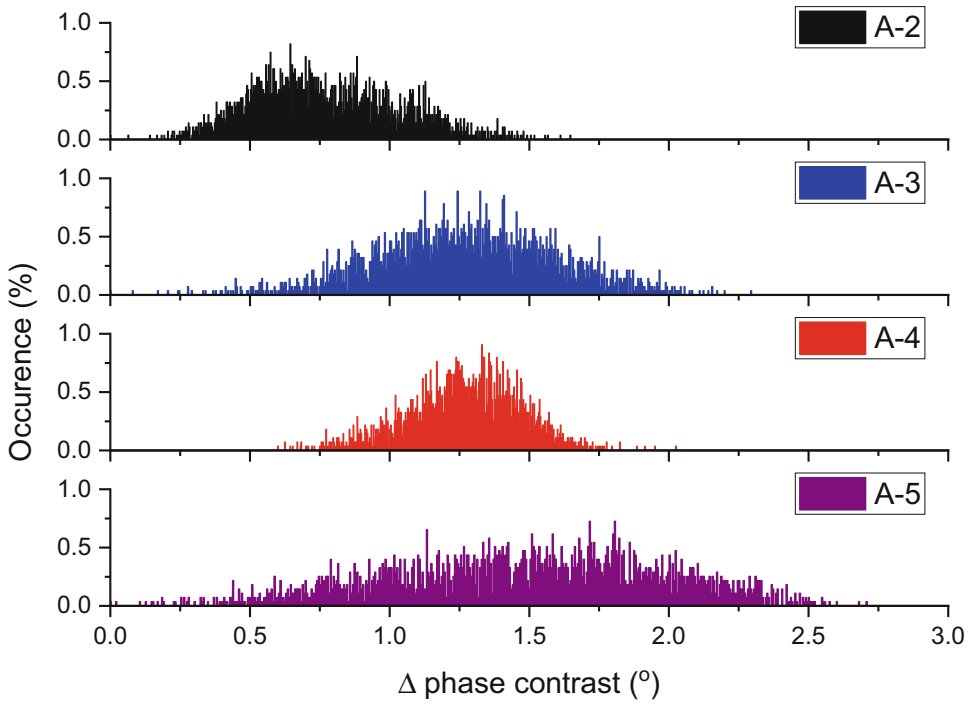

Fig. 9: Statistical histograms of phase contrast difference obtained from bearing analysis of all samples as indicated in the graph

phase images of these coating surfaces are shown in Fig. 8.

As can be seen in the phase images, areas with different phase contrast are present in all coating surfaces. The surface morphology of the samples can be described as domains with low phase contrast dispersed in a continuous network with high phase contrast. The low phase contrast spherical domains are attributed to consist of mainly the acrylic dispersion particles, due to the low T_g of the polymer used in this study. The high phase contrast domains are materials enriched in crosslinker, as the crosslinked network has

higher elasticity compared to the non-crosslinked polymer materials. This typical morphology is in line with the findings from previous study of similar systems,[10] and is believed to result from the initial interaction between the carboxyl groups located at the exterior of the acrylic dispersion particles and the aziridine functionalities from the crosslinker molecules (Fig. 8, schematics, left), followed by the ring opening reaction between the carboxyl and the aziridine functionalities (Fig. 8, schematics, middle), and subsequently further crosslinker diffusion into the dispersion particles and reaction with the carboxyl groups located inside the particles (Fig. 8, schematics, right).

When comparing morphologies among different samples, it is clear that the distribution of acrylic polymer rich domains (low phase contrast) as well as the crosslinker rich domains (high phase contrast) is not the same when different crosslinkers are used. To better visualize this difference in materials distribution, bearing analysis has been carried out in which the highest phase contrast determined from the image was defined as point 0 and the difference between each individual data point and point 0 is then plotted as statistical histograms. This analysis was performed on the phase images from all samples and the obtained histograms are shown in Fig. 9.

As shown in the histograms, the phase contrast distributions vary among samples crosslinked with **A-2** – **A-5**, indicating differences in homogeneity of materials distribution in the coating surfaces. In the case of a coating formulated with **A-2**, the whole histogram is shifted towards lower phase contrast difference (average Δphase contrast: 0.77°), i.e. higher overall phase contrast. This indicates a higher elasticity compared to the other samples (average Δphase contrast **A-3**: 1.27°; **A-4**: 1.27°; **A-5**: 1.48°), which may be related to the different molecular structure of the crosslinks created by **A-2**. Furthermore, when comparing the widths of the distribution, it can be seen that the value of full width at half maximum (FWHM) in the distribution of sample **A-4** (0.38°) and of sample **A-3** (0.58°) are significantly lower than the FWHM of sample **A-5** (1.31°). This is indicative of a more homogeneous distribution of crosslinker **A-4** as a result of its hydrophilic nature. In the case of **A-3**, the less hydrophilic crosslinker molecules distribute slightly less uniformly over the coating, creating a somewhat broader materials distribution. However, when crosslinker **A-5**, which does not contain any stabilizing moieties, is used, the distribution of phase contrast is significantly broader as a result of a rather heterogeneous distribution of the crosslinker molecules.

In further investigation, the domain size and amount of acrylic polymer enriched areas (*i.e.,* areas where no or little crosslinker is present – low phase contrast) are determined from image analysis performed on the phase images. A 200 nm by 200 nm box was drawn in the phase image and a threshold based on the phase contrast distribution was applied to separate the low and high phase contrast domains (Fig. 10a). The average area fraction (based on three randomly selected areas) and average domain size of the acrylic polymer rich materials are then determined and shown in Fig. 10b and c.

By analyzing the area fraction and domain size of the acrylic polymer rich (*i.e.,* non-mixed) materials, the mixing between the acrylic polymer and crosslinker molecules is assessed. As seen in Fig. 10b, the area fraction of acrylic polymer rich materials is higher in sample crosslinked with **A-5**, which results from lower miscibility between the two components, while the sample with **A-3** and **A-4** have similar degree of mixing as evidenced by a lower area fraction of non-crosslinked material. Interestingly, the degree of mixing as indicated by domain area fraction is also roughly similar to the sample crosslinked with **A-2**, a low molecular weight crosslinker that is highly miscible and delivers industry standard crosslinking performance.

The difference in miscibility of crosslinker molecules **A-2** – **A-5** and the acrylic binder phase is further evidenced in the size of the acrylic polymer rich materials domains. In Fig. 10c, the average sizes of low phase contrast domains of different samples are plotted. For reference, in the same graph the average diameter of the acrylic dispersion particles (as obtained by DLS) is displayed as a horizontal line. The difference between the particle diameter and the domain size is then ascribed to the diffusion or penetration depth of crosslinker molecules. Here, we observe that low molecular weight crosslinker, **A-2**, has the highest diffusion, closely followed by **A-4**, with its hydrophilic moieties promoting diffusion into the acrylic polymer, while the diffusion of **A-3** into the particles is somewhat more limited due to its less hydrophilic nature. Lastly the domain size in sample **A-5** is close to the diameter of the acrylic dispersion particles, suggesting that crosslinking reaction mainly takes place between the particles, not inside the particles. This difference in diffusion and distribution of crosslinker molecules could have an impact on the performance of the prepared coatings, which will be examined in the following section.

Application testing

The added value of any crosslinker is determined by the improvement in functional coating, adhesive or other properties that it can deliver. As already suggested by the measurement of crosslinking efficiency, polymeric aziridines can also convey performance benefits matching traditional aziridine products. For example, when used as a crosslinker in a furniture coating formulation containing the versatile high-solids acrylic dispersion Neocryl® XK-117, polymeric aziridine **A-3** can be observed to give a similar performance profile to **A-2** (Table 2). The hardness, thermal and chemical resistance compared to the reference formulation are considerably improved, while the good adhesion properties of this system are retained.

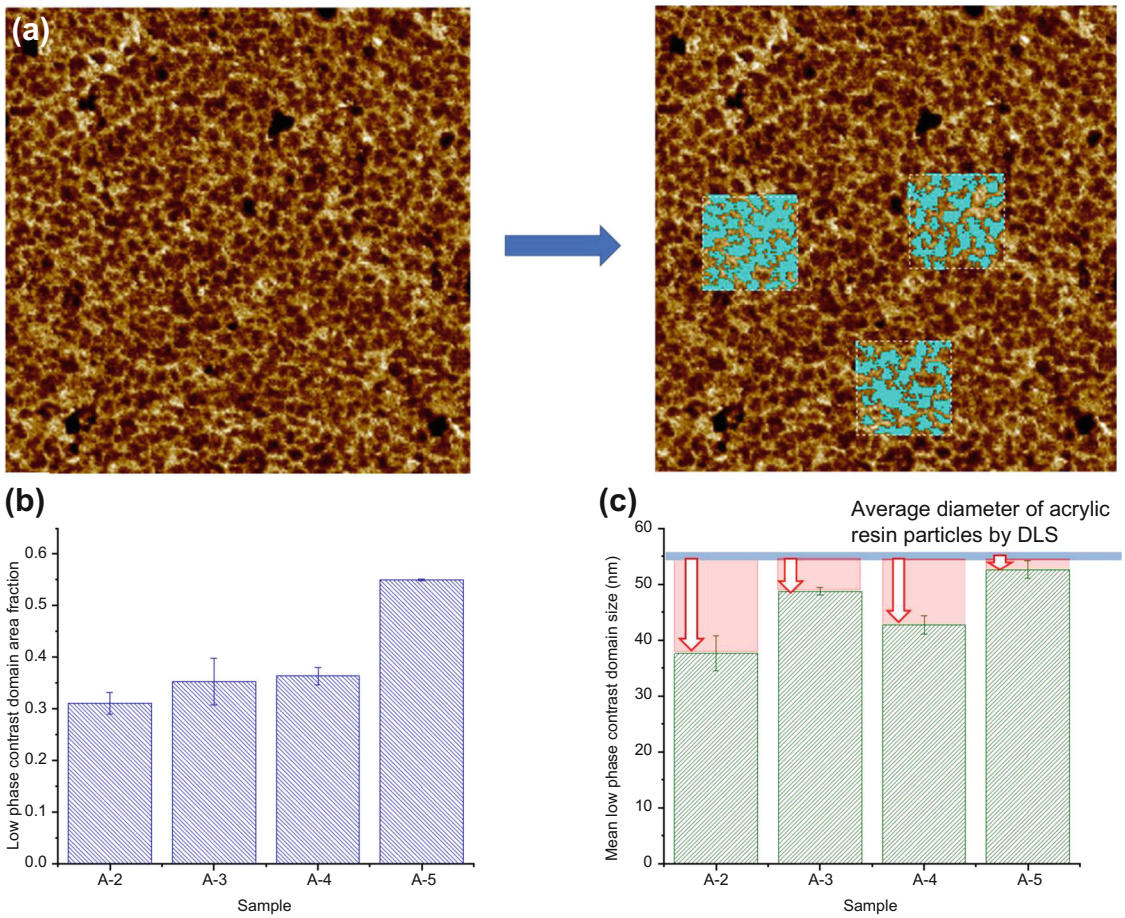

Fig. 10: (a) An example of image analysis performed on AFM phase image of sample A-5: three areas of 200 nm x 200 nm where the low phase contrast domains are highlighted are selected randomly and are shown in the image. (b) The low phase contrast domain area fraction; and (c) the low phase contrast domain average size is determined based on the image analysis. The difference between low phase contrast domain size and the average diameter of the acrylic resin particles is ascribed to the diffusion of crosslinker molecules (indicated by downward block arrows)

A comparison of the more hydrophobic polymeric aziridine crosslinker **A-3** and the more hydrophilic type **A-4** shows that, despite the differences in behavior in aqueous dispersion, both crosslinkers deliver large improvements in functional properties. When formulated in a wood lacquer based on polyurethane dispersion Neorez® R-2005, both crosslinked coatings display significantly better mechanical and chemical resistance characteristics while retaining good optical and drying properties (Table 3).

Conclusions

Polymeric aziridines have been introduced as a new avenue for crosslinking carboxylic waterborne binders. Synthesis of this class of crosslinkers was performed by combining a β-hydroxyalkyleneaziridine intermediate and optionally a stabilizing moiety with a polyfunctional isocyanate backbone. The resulting polymeric aziridines were shown to be non-genotoxic, using the ToxTracker® assay as well as legacy microbiological tests. Coating compositions comprising various aziridines were subjected to mechanical testing, and showed comparable crosslink densities for polymeric and classical aziridines. Additionally, morphological analysis by DLS and AFM demonstrated that by optimizing the stabilizing moiety, compatibility with aqueous compositions and miscibility with acrylic binders can be facilitated for polymeric aziridines. Finally, the functional crosslinking performance of both hydrophilic and hydrophobic polymeric aziridines was confirmed, displaying excellent chemical resistance, mechanical properties and adhesion in application testing.

Acknowledgments The authors would like to thank Covestro for permission to publish this paper. Dr. Rob le Fèbre and Martin Fijten are acknowledged for assistance with DMTA and TTS measurements. The

Table 2: Application testing results of aziridines in furniture coating formulation

Industrial wood coating: XK-117 based formulation

Crosslinker		None	A-2	A-3
Crosslinker loading	% w/w	0	2	2
König hardness				
1-Day cure at 50°C	(s)	64	71	90
Thermal resistance				
Hot Pan		2	5	5
Adhesion				
Beech Gitterschnitt		5	5	5
Beech Crosscut		5	5	5
PVC Gitterschnitt		5	5	5
PVC Crosscut		5	5	5
Chemical resistance				
Test chart: 1-day cure at 50°C (0 = poor, 5 = excellent)	Water, 24 h	2	5	5
	Ethanol, 1 h	1	4	5
	Coffee, 1 h	3	5	5
	Red wine, 6 h	2	5	5
	Sum	**8**	**19**	**20**

Table 3: Application testing results of polymeric aziridines in wood lacquer

Wood lacquer: R-2005 based formulation

Crosslinker		None	A-3	A-4
Crosslinker loading	% w/w	0	6	6
Appearance/drying				
Gloss	(20°/60°/85°)	67/90/98	58/85/98	66/91/99
Dust free time	(min)	18	18	16
Tack free time	(min)	21	21	20
Mechanical performance				
Scratch resistance	(0 = poor, 5 = excellent)	3	4	4
MEK double rubs	–	15	110	110
Stain tests on Leneta chart				
Test chart: 1-day cure at 50°C (0 = poor, 5 = excellent)	Water, 24 h	0	4	4
	Ethanol 48%, 1 h	0	5	4
	Ammonia 25%, 2 min	1	5	5
	Coffee, 1 h	2	2	2
	Hand cream, 6 h	4	4	4
	Sum	**7**	**20**	**19**

authors would like to thank Caroline Dekkers, Wendy van Bavel, Anita van Doorn and Dennis van Opstal for assistance with application testing.

References

1. Tennebroek, R, van der Hoeven-van Casteren, I, Swaans, R, van der Slot, S, Stals, PJM, Tuijtelaars, B, Koning, C, ''Water-Based Polyurethane Dispersions.'' *Polym. Int.*, **68** 832–842 (2019)
2. Weiss, KD, ''Paint and Coatings: A Mature Industry in Transition.'' *Prog. Polym. Sci.*, **22** 203–245 (1991)
3. Schotman, AHM, ''Mechanism of the Reaction of Carbodiimides with Carboxylic Acids.'' *Recl. Trav. Chim. Pays-Bas*, **110** 319–324 (1991)
4. Coogan, RG, ''Post-Crosslinking of Water-Borne Urethanes.'' *Prog. Org. Coat.*, **32** 51–63 (1997)
5. Harmsen, AS, Jansse, PL, Vermeer, M, van de Hoogen, E, van der Werf-Willems, N, ''Crosslinking Mechanisms.'' *Eur. Coat. J.*, **05** 14–26 (2003)
6. Roesler, RR, Danielmeier, K, ''Tris-3-(1-aziridino)propionates and Their Use in Formulated Products.'' *Prog. Org. Coat.*, **32** 51–63 (2004)
7. Bückmann, AJP, Overbeek, GC, Scheerder, J, Stals, PJM, van Dijk, SJ, van der Zwaag, D, ''Aqueous Crosslinkable Coating Composition.'' WO Patent 016168, 2019
8. Hendriks, G, Derr, RS, Misovic, B, Morolli, B, Calléja, FMGR, Vrieling, H, ''The Extended ToxTracker Assay Discriminates Between Induction of DNA Damage, Oxidative Stress, and Protein Misfolding.'' *Tox. Sci.*, **150** 190–203 (2016)
9. Taylor, JW, Winnik, MA, ''Functional Latex and Thermoset Latex Films.'' *J. Coat. Tech. Res.*, **1** 163–190 (2004)
10. Bückmann, AJP, Cronin, J, Overbeek, GC, Stals, PJM, van der Zwaag, D, ''Benign and Efficient Crosslinking.'' *Eur. Coat. J.*, **12** 34–43 (2020)